International Journal on
"Technical and Physical Problems of Engineering"
(IJTPE)
Published by International Organization of IOTPE

ISSN 2077-3528
IJTPE Journal
www.iotpe.com
ijtpe@iotpe.com

March 2024	Issue 58	Volume 16	Number 1	Pages 284-291

PREDICTING TORSIONAL BEHAVIOR IN Z-SHAPED TWISTING METAMATERIALS

A. Barhoumi [1] M. Atify [2] G. Ganzosch [3] A. Rahmani [1]

1. Advanced Materials and Applications Laboratory (LEM2A), Moulay Ismail University, Meknes, Morocco
a.barhoumi@edu.umi.ac.ma, ab.rahmani@umi.ac.ma
2. Department of Innovation and Smart Technologies (IST), Polydisciplinary Faculty, Sultan Moulay Slimane University, Beni Mellal, Morocco, atifym@gmail.com
3. Institute of Mechanics, 5th Faculty, Berlin University of Technology, Berlin, Germany
gregor.ganzosch@rwth-aachen.de

Abstract- Compression-torsion mechanical metamaterials represent a significant advance in the conversion of axial compressive (or tensile) loads into rotational movements. This additional degree of freedom, non-existent according to linear Cauchy elasticity, is due to the chiral effects of the structure allowed in the context of Eringen micropolar continuum mechanics. The use of Machine Learning (ML) in microstructure design has revolutionized this field of research, enabling substantial time savings in simulation and sample experimentation. In the present manuscript, a twisting metamaterial belonging to the Z-structures and built around a unit cell composed of two diamond-shaped lattices has been studied. In this type of metamaterial structure, the overall torsion is closely related to the morphology and dimensions of the cell, and by changing its intrinsic geometric parameters, a variety of eighteen thousand finite element models were generated. Then, using Machine Learning, we were able to predict the torsion angles of each combination, and to check the effectiveness of the predicted results, numerical and experimental approaches were combined. The error did not exceed 0.07% when comparing the results of the ML approach and those obtained using finite element simulations (FEM). To validate our results, uniaxial mechanical compression experiments were carried out on specimens manufactured using the stereolithography 3D printing technique. The robustness of the results obtained paves the way for the application of these findings to other Z-shaped metamaterials with similar torsional effects.

Keywords: Compression-Torsion Metamaterial, Machine Learning, Finite Elements Method, Predictive Modeling, Additive Manufacturing.

1. INTRODUCTION

Metamaterials are engineered materials with unconventional effective properties that may go beyond those of the base material [1, 2]. Mechanical metamaterials are one such family [3-5]. They can exhibit negative or zero Poisson's ratio [6], negative compressibility [7], excellent resistance to indentation [8] and compression-induced torsion [9-12]. The latter behavior, which consists in transforming a compressive or tensile axial load into a twist, has recently attracted the interest of many researchers, especially with the advent of additive manufacturing, also known as three-dimensional (3D) printing. The overall twist angle of the metamaterial structure depends on that of the unit cell and the number of cells assembled horizontally and vertically [13]. The cell itself is optimized in terms of its intrinsic geometrical parameters: height, side length, thickness, etc.

It's worth pointing out that there are two types of approach to the study of mechanical metamaterials. The first, known as inverse design, consists in designing metamaterial structures to satisfy target properties, and the second in precisely determining the mechanical characteristics of the designed models. Due to its complexity, inverse design is usually supported by optimization methods to determine optimal design parameters and then evaluate them through simulations such as finite element analysis (FEA). This evaluation becomes a very slow and costly task, and could last days or even longer in the case of mechanical metamaterials due to the large number of parameters involved in the targeted solution, as this methodology requires all parameters to be updated after each response calculation.

Lately, given the large number of factors involved and the complexity of resolution in terms of time, memory and computer speed, the use of the artificial intelligence (AI) approach has become a necessity, particularly for predicting results. The combination of AI and optimization for the design of mechanical metamaterials is in great demand in this and other areas of research. Chang, et al. [14] designed an auxetic metamaterial with zero Poisson's ratio by developing a machine learning (ML) model combining an artificial back-propagation neural network and a genetic algorithm. Adil, et al. [15] also used machine learning ML to predict the absorptivity of L-shaped metamaterials.

Registered: 231218 Article Info: 1738 Accepted: 230230
Reserved: 240219 Available: 240331

Mansouri, et al. [16] applied AI in the electrical field, to improve the performance of a nonlinear controller using the SVPWM technique. In robotics, Atify, et al. [17] used this approach to determine the optimal positions for moving a hexapod robot. This method requires solving a set of nonlinear equations, which is very time-consuming. The AI approach has overcome this problem. The AI approach is also applied to the prediction of results based on information gathered in a database table. Lakhdar, et al. [18] used AI to compare it with the finite element method in order to find the most suitable method for better modeling the behaviors of PVC bio-loaded with chicken feathers, and then predicting the behaviors with different percentages of bio-loading. As for Outemsaa, et al. [19], they compared the accuracy of the prediction of the roughness of a machined surface by artificial intelligence and by statistical model.

In this paper the prediction of the twist angle within a Z-shaped unit cell of a metamaterial that comprises two diamond-shaped lattices is determined by the artificial intelligence approach based on a data table that takes into consideration its intrinsic characteristics. A neural network model is used to model the structure. A gradient descent algorithm is applied to determine the best network parameters, which minimize the errors between the results given by the model and the true values of the outputs given by the data table. The results obtained were confirmed by both simulations and experiments. A Python program was developed to generate no less than eighteen thousand combinations. These represent finite element models with a variety of geometric parameters. The resulting deep learning model (DL) predicts, with a high degree of accuracy, the torsion angle corresponding to a given geometric design.

2. ARTIFICIAL INTELLIGENCE APPROACH

2.1. Unit Cell Structure

Our study will focus on the unit cell shown in Figure 1, the result of a previous optimization study [20]. It involves the assembly of two rhombic shaped lattices by four identical rods inclined at an angle θ to the horizontal plane.

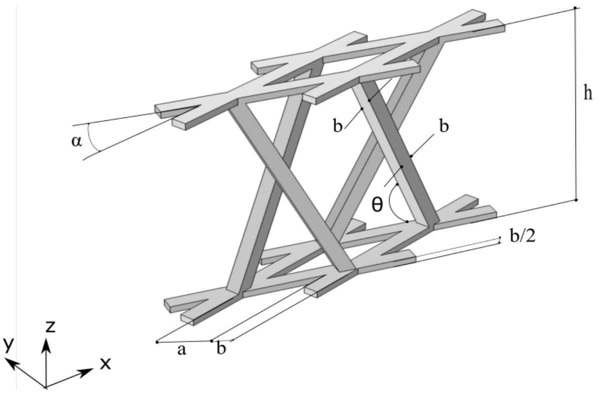

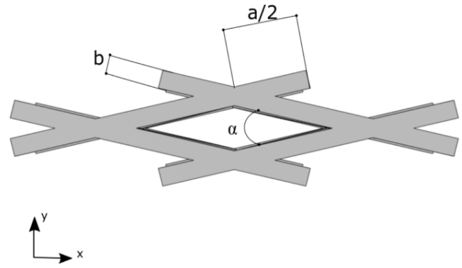

Figure 1. Isometric and top views of the unit cell [20]

The chiral way in which they are arranged gives the entire structure the ability to twist under tensile or compressive load. The rest of the physical and geometric parameters are listed in Table 1.

Table 1. Physical and geometrical parameters of the unit cell

a (mm)	h (mm)	b (mm)	E (GPa)	v	θ (°)	α (°)
12	24	1.5	2.61	0.4	63.44	20

2.2. Machine Learning

2.2.1. Dataset

The artificial intelligence approach consists in solving a problem by learning (Machine learning ML), this learning is established by examples that are grouped together in a table (Dataset). This table contains as inputs the parameters of the problem and their corresponding outputs, i.e. in the database we have the parameters α, h, a, b and θ (inputs) and their outputs β (results that are known). The database must be significant to obtain good results. In our case, Table 2 represents a sample of the database applied to solve the problem.

Table 2. Sample Dataset

α (°)	h (mm)	a (mm)	b (mm)	θ (°)	β (°/%)
92	24	12	1.5	63.44	4.516
40	30	12	1.5	68.20	12.320
70	42	12	1.5	74.05	17.500
80	50	7.5	2	81.47	0.020
75	10	8	1	51.34	2.200
80	41	3.1	1.5	85.68	0.001
65	24	12	1.5	63.44	4.844
90	24	15	3	57.99	4.123
90	38	5	1.5	82.5	19.820

2.2.2. Neural Network Model

The learning method used for Machine Learning (ML) solving is the neural network. This consists in placing hidden layers between inputs and outputs containing linked neurons. Figure 2 shows an elementary single-neuron network with output σ defined by the sigmoid activation Equation (1). Whereas the intermediate function Z is expressed by the Equation (2).

$$\sigma(Z) = \frac{1}{1+e^{-Z}} \tag{1}$$

$$Z = X_1 \times W_1 + X_2 \times W_2 + b \tag{2}$$

where, X_1 and X_2 are the input parameters, W_1 and W_2 are the link weights and b are the neuron bias.

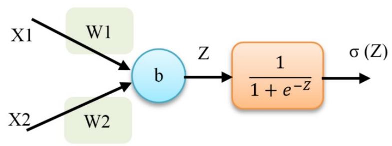

Figure 2. Neural network with sigmoid activation function

Figure 3 displays a neural network containing two hidden layers and three neurons. The expression of Z_3 is illustrated by Equation (3), such that Z_1 and Z_2 are given by Equations (4) and (5), respectively.

$$Z_3 = Z_1 \times W_{31} + Z_2 \times W_{32} + b_3 \tag{3}$$

$$Z_1 = X_1 \times W_{11} + X_2 \times W_{12} + b_1 \tag{4}$$

$$Z_2 = X_1 \times W_{21} + X_2 \times W_{22} + b_2 \tag{5}$$

The objective of the network is to retrieve the best values of the weights W and the biases b that verify the database as much as possible, i.e., to minimize the error between the true values given in the table and the results retrieved by the neural network through the weights W and the biases b.

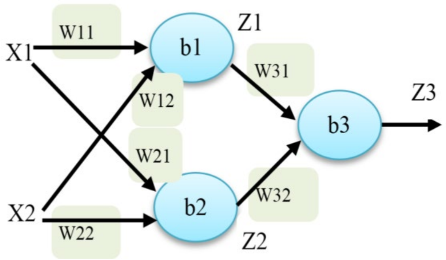

Figure 3. Three neurons with two hidden layers

In our case, the neural network applied is illustrated in Figure 4, and includes 2 hidden layers in addition to the output layer, with 32, 16 and 1 neurons respectively. The network shows the five inputs (α, h, a, b and θ), and the output β. The activation functions used are the sigmoid functions for the first two hidden layers and the linear function for the last layer.

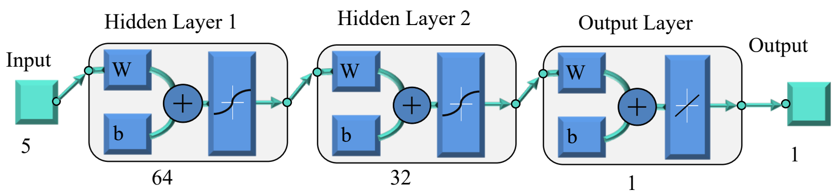

Figure 4. Neural network diagram

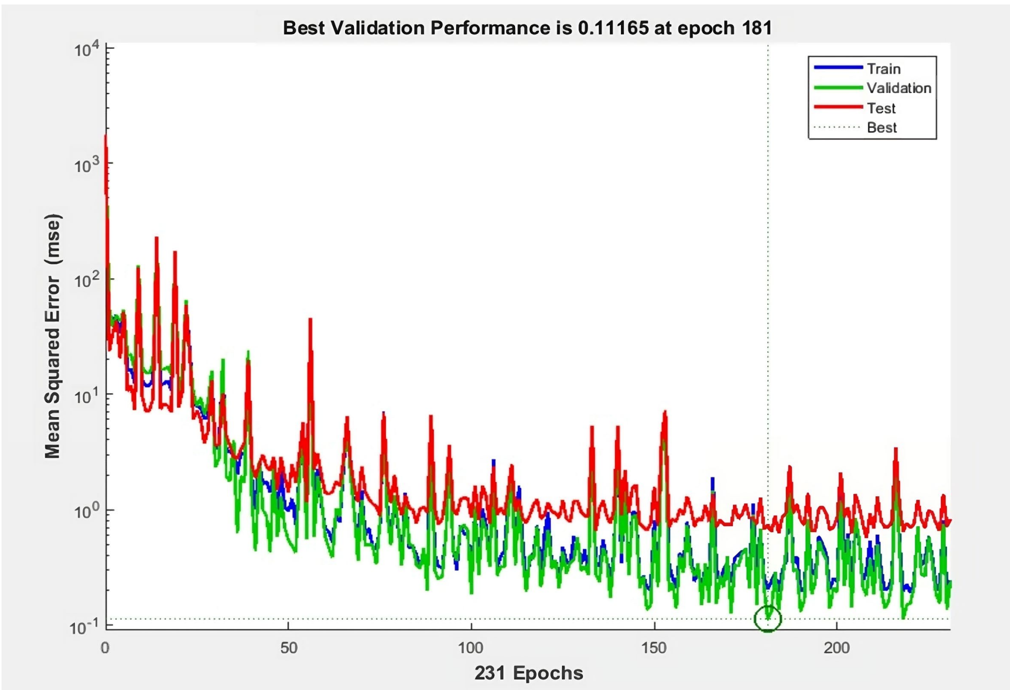

Figure 5. Validation performance curves

In order to minimize the error between the values given in the table and the results given by the neural network, we apply the gradient descent algorithm, which consists of choosing random values for the parameters W and b, then calculating the error between the true values of the outputs and the results given by the neural network as a function of the initial values of W and b, and finally updating the values of the weights (W) and biases (b). This process is repeated until the best values for weights W and biases b have been determined.

2.3. Validation of Results

2.3.1. Validation with Performance Curves

For verification and subsequent validation of the applied neural network, the error is obtained from the performance curves shown in Figure 5. If the given error is acceptable, the program is validated, in which case the applied neural network will replace the entire data table. In addition, this network is used to predict results for inputs that are not given in the data table, this is prediction by Machine Learning. The performance curves found for our program are displayed in Figure 5.

2.3.2. Test Table

For program validation, another table is given: the test table. The outputs of this table are not given to the neural network, but are kept hidden. The program is then asked to find the outputs, and the total error between the predictions given by the neural network and the true values that were hidden is calculated. Table 3 lists part of the test table used to verify our neural network. The True_β column corresponds to the true values of the outputs that were hidden, while the Predict_β column represents the values of the beta angle given by the neural network. We deduce that the errors between the results predicted by the neural network and the true results are very acceptable indeed, and the program is therefore validated.

Table 3. Prediction result

α (°)	h (mm)	a (mm)	b (mm)	θ (°)	True_β (°/%)	Predict_β (°/%)
69	24	12	1.5	63.44	4.724	4.722
92	24	12	1.5	63.44	4.516	4.514
90	24	15	2.5	57.99	4.273	4.265
90	24	15	4.5	57.99	3.574	3.570
90	28	15	1.5	61.82	4.532	4.532
90	30	15	4.5	63.43	3.918	3.914
90	32	15	3.0	64.88	4.338	4.348
40	30	12	1.5	61.19	12.32	12.23

3. NUMERICAL AND EXPERIMENTAL VALIDATION

3.1. Simulation

To verify the effectiveness of the predicted results, finite element simulations were first carried out using COMSOL Multiphysics software. Three models were chosen with the same physical characteristics of the base material, such as Young's modulus E =2.61 GPa and Poisson's ratio ν = 0.4, while the other geometric parameters were as follows: α =30° or 45° or 60°, a=12 mm, h=24 mm and b=1.5 mm.

The study focuses on the reversible elastic domain due to the low deformations observed. A uniaxial load is applied to displace the upper face of the models with a relative uniaxial compressive strain set at 1%, while the lower boundary remains stationary. Torsion angles are calculated at displacements in x and y directions. In order to guarantee the mesh-independence of the numerical simulations, a mesh sensitivity analysis was carried out beforehand.

The deformation of an example cell with α=60° is shown in Figure 6. Knowing that two consecutive angles of a rhombus are supplementary, each specific angle α corresponds to another angle (π-α). Consequently, this doubles the number of samples, totaling six angles: 30°, 45°, 60°, 120°, 135° and 150°.

All the results found are listed in Table 4. Comparing them with the results of the Machine Learning approach, we find that the error is very small, of the order of 0.07% at most.

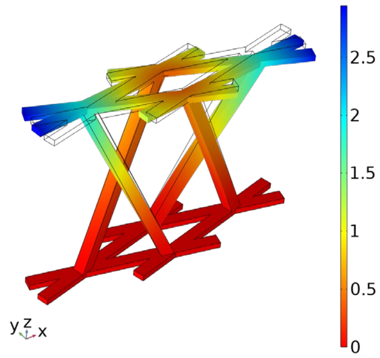

Figure 6. Deformation image of an example cell having α =60° along z-direction, ε=1%

Table 4. Comparison of predicted and simulated torsion angles

α (°)	h (mm)	a (mm)	b (mm)	θ (°)	Twist β by FEM (°/%)	Predicted β twist (°/%)	Error
30	24	12	1.5	63.44	7.702	7.706	0.04%
45	24	12	1.5	63.44	5.949	5.950	0.01%
60	24	12	2.5	63.44	5.028	5.032	0.07%
120	24	12	1.5	63.44	5.028	5.032	0.07%
135	24	12	1.5	63.44	5.949	5.950	0.01%
150	24	12	1.5	63.44	7.702	7.706	0.04%

3.2. Experimentation

The compression-torsion effect is then examined in more detail experimentally, in order to validate our numerical results and those predicted by the Machine Learning program. The specimens shown in Figure 7 are fabricated using stereo-lithographic appearance (SLA) technology, and the Form 2 3D printer from US manufacturer Formlabs was used. It is worth emphasizing that all unit cells are manufactured, as shown in Figures 8 and 9, with a layer of mirror symmetry in the middle to avoid friction between the upper and lower faces of the samples with the loading platforms during compression.

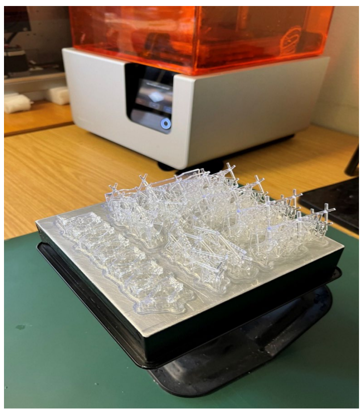

Figure 7. Form 2 (3D) printer and fabricated experimental samples

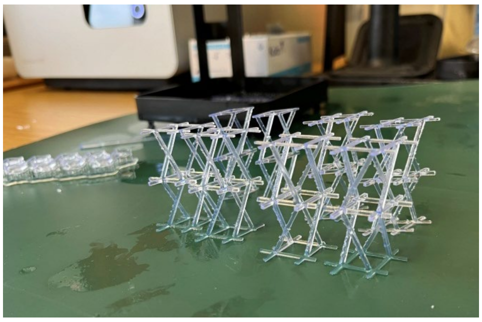

Figure 8. Fabricated experimental samples

In addition to the metamaterial cells needed to validate the results, two standard dog-bone-shaped samples, in accordance with ISO527-1(2012) [21] , were printed simultaneously to obtain the mechanical properties of the UV-cured EPOXY resin. The printing layer thickness was 100 µm. These properties were used for finite element analysis of the structures. It is interesting to note that other constituent materials with wide elastic domains can be used, as their mechanical properties have a negligible effect on compression-induced torsion [12], [22].

As shown in Figures 10 and 11, all specimens are first pixelated by paint spraying, so that the two-dimensional digital image correlation (2D-DIC) technique can later be used for deformation measurements. Tests are carried out on a "Zwick Roell" tensile/compression machine with a load capacity of 2.5 kN. According to the above-mentioned standard, the average values of Poisson's ratio and Young's modulus calculated are 0.39 and 2.58 GPa, respectively. The remaining specimens are then compressed on the same machine, applying a quasi-static compression displacement at a loading speed of 3 mm/min. The lower head remains fixed. During the test, a digital camera (Canon EOS M6 Mark II) was aimed at the mirror layer to capture an image every 0.1 mm of longitudinal deformations and record them. Figure 11 shows the experimental setup.

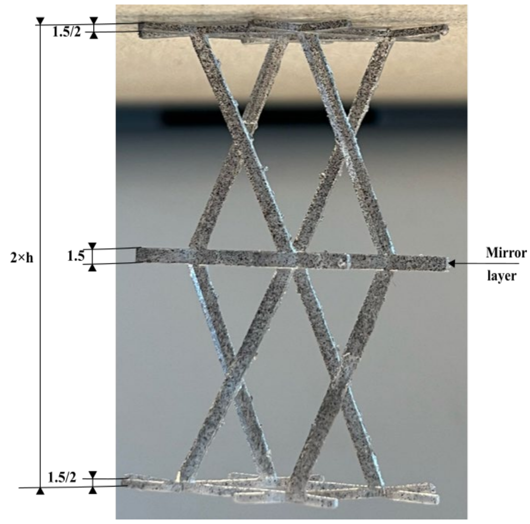

(a)

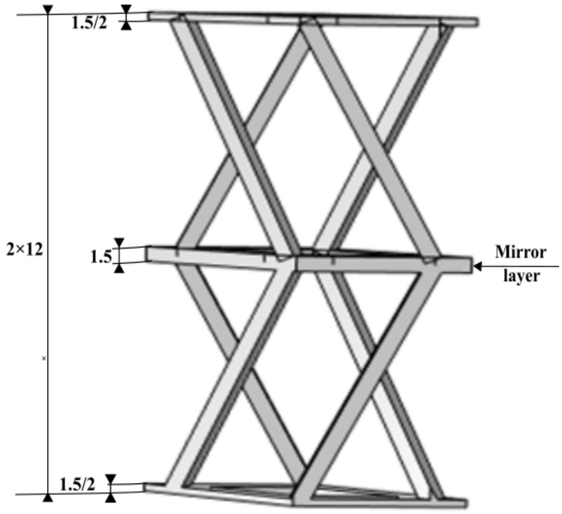

(b)

Figure 9. Unit cell with a mirror plane, all dimensions in mm, a) The as-printed specimen, b) CAD model

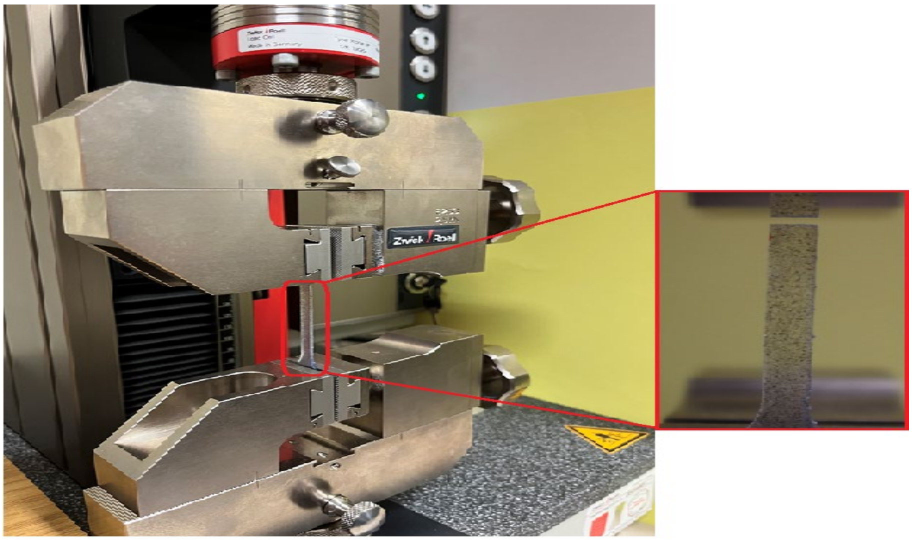

Figure 10. Uniaxial tensile testing of dog bone samples

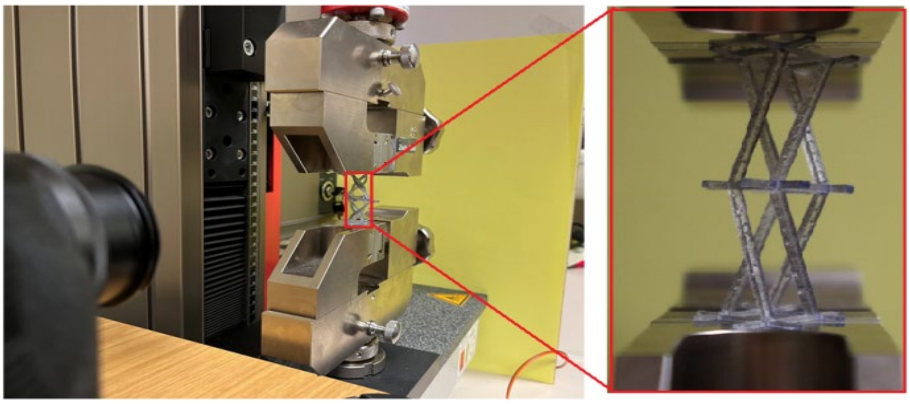

Figure 11. The experimental setup

The sketch in Figure 12 illustrates that, when the sample is twisted, point P moves towards point M. The distance between the center of the sample (point O) and point P is L, which can be calculated as a function of side a and angle α by Equation (6). Obviously, in our application, the 2D-DIC technique could not directly evaluate the displacement Δx. Thus, the following Equation (7) for the torsion angle β of the midplane depends only on the intrinsic cell parameters and the displacement Δy.

$$L = a \times \cos(\frac{\alpha}{2}) \quad (6)$$

The twist angle β of the sample is translated into the rotation of point P at point M, as shown in the sketch in Figure 12. The twist is then calculated by Equation (7).

$$\beta = \left(\frac{180}{\Pi}\right) \times \arcsin\left(\frac{\Delta y}{a \times \cos(\frac{\alpha}{2})}\right) \quad (7)$$

The values Δx and Δy represent the distances between point P and point M, measured along the x and y axes, respectively, and the side length of the rhombus a=12mm. A further comparison is made between the experimental and numerical approaches. As indicated in Table 5, we find that the error does not exceed 5.51%, which is largely acceptable and allows us to validate our models.

Moreover, although we focus here on a unit cell composed of two rhombic-shaped lattices, the present approach can be extended to other Z-shaped metamaterials with compression-torsion effect without any difficulty.

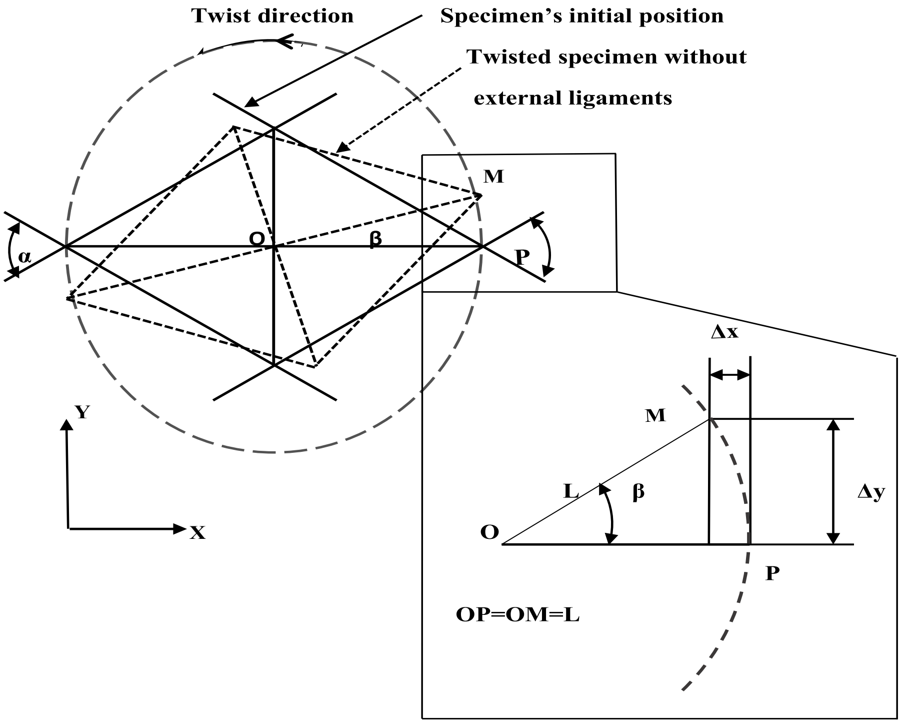

Figure 12. Top view sketch of twisted unit cell

Table 5. Comparison of experimental and numerical torsion angles

α (°)	h (mm)	a (mm)	b (mm)	θ (°)	Twist β by FEM (°/%)	Twist β by EXP (°/%)	Error
30	24	12	1.5	63.44	7.702	7.3	5.51%
45	24	12	1.5	63.44	5.949	5.7	4.37%
60	24	12	2.5	63.44	5.028	5.3	5.12%
120	24	12	1.5	63.44	5.028	5.3	5.12%
135	24	12	1.5	63.44	5.949	5.7	4.37%
150	24	12	1.5	63.44	7.702	7.3	5.51%

4. CONCLUSIONS

Chirality in elastic mechanical metamaterials emphasized the existence of an additional rotational degree of freedom induced by compression or tension. Lately, the combination of artificial intelligence and optimization in the design of microstructures for mechanical metamaterials is highly sought-after in this field of research, due to the substantial time saved in simulation and sample experimentation. In the present work, the Machine Learning approach has been used to predict the compression-induced torsion angles of a twisting metamaterial belonging to Z-structures and built around a unit cell composed of two diamond-shaped lattices. The study is limited to the reversible elastic domain with a relative uniaxial compressive strain fixed at 1%. By varying the intrinsic geometric parameters of the unit cell, a Python program generated some eighteen thousand combinations, and the predictions given by the algorithm proved satisfactory.

To verify the effectiveness of the predicted results, simulations were carried out on a series of numerical models using COMSOL Multiphysics software to study the influence of unit cell geometry on twist angle. The error did not exceed 0.07% when comparing the results of the Machine Learning approach and those obtained by finite element simulation (FEM). Finally, to validate the results of our study, uniaxial compression tests were carried out on samples manufactured using the 3D stereolithography printing technique. The consistency of the numerical and experimental results was clearly demonstrated by a maximum error of 5.51%. The relevance of the present approach means that it can be applied to other Z-shaped compression-torsion metamaterials.

REFERENCES

[1] N.I. Zheludev, "The Road Ahead for Metamaterials", Science, Vol. 328, No. 5978, pp. 582-583, April 2010.
[2] A.A. Zadpoor, M.J. Mirzaali, L. Valdevit, J.B. Hopkins, "Design, Material, Function, and Fabrication of Metamaterials", APL Materials, Vol. 11, No. 2, p. 020401, February 2023.
[3] K. Muamer, T. Buckmann, R. Schittny, M. Wegener, "Metamaterials Beyond Electromagnetism", Reports on Progress in Physics, Physical Society (Great Britain), Vol. 76, p. 126501, November 2013.
[4] K. Bertoldi, V. Vitelli, J. Christensen, M. van Hecke, "Flexible Mechanical Metamaterials", Nat. Rev. Mater, Vol. 2, No. 11, p. 17066, November 2017.
[5] Z. Huang, G. Shao, L. Li, "Micro/Nano Functional Devices Fabricated by Additive Manufacturing", Progress in Materials Science, Vol. 131, p. 101020, January 2023.
[6] M. Fu, F. Liu, L. Hu, "A Novel Category of 3D Chiral Material with Negative Poisson's Ratio", Composites Science and Technology, Vol. 160, pp. 111-118, May 2018.
[7] R.H. Baughman, S. Stafstrom, C. Cui, S.O. Dantas, "Materials with Negative Compressibilities in One or More Dimensions", Science, Vol. 279, No. 5356, pp. 1522-1524, March 1998.
[8] L.L. Hu, M.Z. Zhou, H. Deng, "Dynamic Indentation of Auxetic and non-Auxetic Honeycombs under Large Deformation", Composite Structures, Vol. 207, pp. 323-330, 2019.
[9] T. Frenzel, M. Kadic, M. Wegener, "Three-Dimensional Mechanical Metamaterials with a Twist", Science, Vol. 358, No. 6366, pp. 1072-1074, November 2017.
[10] W. Xu, Z. Liu, L. Wang, P. Zhu, "3D Chiral Metamaterial Modular Design with Highly-Tunable Tension-Twisting Properties", Materials Today Communications, Vol. 30, p. 103006, March 2022.
[11] W. Xu, L. Wang, Z. Liu, P. Zhu, "General Assembly Rules for Metamaterials with Scalable Twist Effects", International Journal of Mechanical Sciences, Vol. 259, p. 108579, December 2023.
[12] B. Lemkalli, M. Kadic, Y.E. Badri, S. Guenneau, A. Bouzid, Y. Achaoui, "Mapping of Elastic Properties of Twisting Metamaterials onto Micropolar Continuum Using Static Calculations", International Journal of Mechanical Sciences, p. 108411, April 2023.
[13] R. Zhong, M. Fu, X. Chen, B. Zheng, L. Hu, "A Novel Three-Dimensional Mechanical Metamaterial with Compression-Torsion Properties", Composite Structures, Vol. 226, p. 111232, October 2019.
[14] Y. Chang, H. Wang, Q. Dong, "Machine Learning-based Inverse Design of Auxetic Metamaterial with Zero Poisson's Ratio", Materials Today Communications, Vol. 30, p. 103186, March 2022.
[15] M. Adil, "Utilizing Machine Learning Techniques for Predictive Modelling of Absorptivity in l-Shaped Metamaterials", Presented at the Advanced Topics in Mechanics of Materials, Structures and Construction, pp. 656-665, September 2023.
[16] A. Mansouri, I. El Myasse, A.E. Magri, R. Lajouad, F. Giri, "Nonlinear Control of Five-Phase PMSG Wind Turbine Connected to Vienna Type Rectifier Using SVPWM", The 3rd International Conference on Innovative Research in Applied Science, Engineering and Technology (IRASET), pp. 1-6, May 2023.
[17] M. Atify, M. Bennani, A. Abouabdellah, "Structure Optimization of a Hexapod Robot", International Journal on Technical and Physical Problems of Engineering (IJTPE), Issue 50, Vol. 14, No. 1, pp. 42-49, March 2022.
[18] A. Lakhdar, A. Moumen, Z. Laabid, K. Mansouri, "Prediction of The Behavior of Bio-Loaded Flexible PVC by Chicken Feathers with Artificial Neural Networks", E3S Web Conf., Vol. 336, p. 00004, 2022.
[19] O. Outemsaa, O.E. Farissi, "Predicting of Tool Path Effect on Roughness of a Machined Surface Using ANN

and RSM", International Journal on Technical and Physical Problems of Engineering (IJTPE), Issue 54, Vol. 15, No. 1, pp. 26-32, March 2023.
[20] A. Barhoumi, B. Lemkalli, H. Jakjoud, Y. Achaoui, A. Rahmani, "Improved Compression-Torsion Conversion in Geometrically Optimized Mechanical Metamaterials", The 2nd International Conference on Innovative Research in Applied Science, Engineering and Technology (IRASET), March 2022.
[21] E. Iso, "527-1. Plastics - Determination of Tensile Properties - Part 1: General Principles", International Organization of Standardization, Geneva, Switzerland, 2012.
[22] L. Wang, H.T. Liu, "3D Compression - Torsion Cubic Mechanical Metamaterial with Double Inclined Rods", Extreme Mechanics Letters, Vol. 37, p. 100706, May 2020.

BIOGRAPHIES

Name: **Abderrahim**
Surname: **Barhoumi**
Birthday: 15.01.1977
Birthplace: Beni Mellal, Morocco
Bachelor: Mechanical Engineering, ENSAM, Mohammed V University, Rabat, Morocco, 1998
Master: Mechanical Engineering, ENSAM, Mohammed V University, Rabat, Morocco, 2019
Doctorate: Student, Mechanical Metamaterials, Department of Physics, Faculty of Sciences, Moulay Ismail University, Meknes, Morocco, 2020
The Last Scientific Position: Teacher, Industrial Engineering Sciences, CPGE Mohamed VI, Kenitra, Morocco, Since 2021
Research Interests: Machine Learning, Modeling, Simulation and Additive Manufacturing of Mechanical Metamaterials
Scientific Publications: 2 Papers

Name: **Mohamed**
Surname: **Atify**
Birthday: 19.10.1978
Birthplace: Boulemane, Morocco
Bachelor: Mechanical Engineering, ENSAM, Mohammed V University, Rabat, Morocco, 2001
Master: Mechanical Engineering, ENSAM, Mohammed V University, Rabat, Morocco, 2016
Doctorate: Robotics and Mechanical Engineering, Engineering Sciences Laboratory, Ibn Tofail University, ENSA, Kenitra, Morocco, 2022
The Last Scientific Position: Assist. Prof., Department of New Technologies, Polydisciplinary Faculty, Sultan Moulay Slimane University, Beni Mellal, Morocco, Since 2024.
Research Interests: Robotics, Artificial Intelligence, Metamaterials
Scientific Publications: 6 Papers

Name: **Gregor**
Surname: **Ganzosch**
Birthday: 13.08.1986
Birthplace: Ratibor, Poland
Bachelor: Design of a Hydraulic Left Mock Heart in a Mock Circulation Loop, Institute of Applied Medical Technology, Department of Cardiovascular Technology, Rhine-Westphalian Technical University, Aachen, Germany, 2013
Master: Small Scale Bone Deformation: A Study of Compression Testing by Simulation, validated by Digital Image Correlation, Department of Cardiovascular Technology, Rhine-Westphalian Technical University, Aachen, Germany, 2015
Doctorate: Design, Manufacturing, and Experimental Analysis of Additively Fabricated Metamaterials with a Pantographic Substructure, Institute of Mechanics, 5th Faculty, Berlin University of Technology, Berlin, Germany, 2022
The Last Scientific Position: Scientific Assistant, Institute of Mechanics, 5th Faculty, Berlin University of Technology, Berlin, Germany, Since 2016
Research Interests: 3D Printing, CAD, Mechanical Behavior of Materials, Micromechanics Mechanical Testing Digital Image Correlation and Tracking, Biomechanical Engineering
Scientific Publications: 17 Papers

Name: **Abdelhai**
Surname: **Rahmani**
Birthday: 06.08.1968
Birthplace: Meknes, Morocco
Bachelor: Physics of Solids, Department of Physics, Faculty of Sciences, Moulay Ismail University, Meknes, Morocco, 1993
Master: Interaction Radiation Matter, Department of Physics, Faculty of Sciences, Ben M'sik Sidi Othmane University, Casablanca, Morocco, 1995
Doctorate: Physic, Elemental Analyzes by X-ray Fluorescence Applications to Geochemistry and Environmental Sciences, Faculty of Sciences, Moulay Ismail University, Meknes, Morocco, 2002
The Last Scientific Position: Prof., Department of Physics, Faculty of Sciences, My Ismail University, Meknes, Morocco, Since 2011
Research Interests: Nanomaterials and Metamaterials, Digital Modeling, Characterization Techniques
Scientific Publications: 46 Papers, 4 Books, 4 Projects, 6 Theses
Scientific Memberships: Montpellier II University, Lille University, Brest University, SPANET